Biosensors and Bioelectronics 26 (2011) 4263–4269

Contents lists available at ScienceDirect

Biosensors and Bioelectronics

journal homepage: www.elsevier.com/locate/bios

Microflow Cytometer for optical analysis of phytoplankton

Nastaran Hashemi, Jeffrey S. Erickson, Joel P. Golden, Kirsten M. Jackson, Frances S. Ligler*

Center for Bio/Molecular Science and Engineering, Naval Research Laboratory, Washington, DC, USA

ARTICLE INFO

Article history:
Received 16 December 2010
Received in revised form 23 March 2011
Accepted 31 March 2011
Available online 30 April 2011

Keywords:
Flow cytometry
Microfluidics
Optical sensing
Hydrodynamic focusing
Phytoplankton

ABSTRACT

Analysis of the intrinsic fluorescence profiles of individual marine algae can be used in general classification of organisms based on cell size and fluorescence properties. We describe the design and fabrication of a Microflow Cytometer on a chip for characterization of phytoplankton. The Microflow Cytometer measured distinct side scatter and fluorescence properties of *Synechococcus* sp., *Nitzschia d.*, and *Thalassiosira p.*; measurements were confirmed using the benchtop Accuri C6 flow cytometer. The Microflow Cytometer proved sensitive enough to detect and characterize picoplankton with diameter approximately 1 μm and larger phytoplankton of up to 80 μm in length. The wide range in size discrimination coupled with detection of intrinsic fluorescent pigments suggests that this Microflow Cytometer will be able to distinguish different populations of phytoplankton on unmanned underwater vehicles.

Published by Elsevier B.V.

1. Introduction

Phytoplankton are marine microorganisms that respond very rapidly to changes in their environment. Alterations in phytoplankton assemblies may reflect environmental changes within a few hours or over much longer periods. As such, changes in phytoplankton populations can be measured in response to introduction of environmental pollutants, alterations in ocean currents, and global climate change (Nehring, 1998; Thyssen et al., 2008). Blooms of some species of phytoplankton, especially in littoral waters, can cause illness to mammals, fish, corals, and other marine organisms (Burk et al., 1998; Harvell et al., 1999; Knap et al., 2002; Landsberg, 2002).

A variety of analytical methods have been deployed to identify changes in populations of marine algae with a view to understanding both the organisms and the forces that impact their proliferation. Remote spectrometry from satellites or from airplanes provides a reflectance spectra based on sunlight or laser light, respectively (Barbini et al., 2006; Churnside and Donaghay, 2009; Fantoni et al., 2006; Fiorani et al., 2007; Hoge et al., 2005). *In situ* spectrometry also provides information on the average population present in the water based on backscatter and/or laser induced fluorescence; while focusing on more local changes than remote analysis from above, laser-induced fluorescence instruments deployed from a ship or buoy still provide only mean values of the backscatter and pigment spectra for all organisms present in the field of view (Drozdowska, 2007). Flow cytometry and cell imaging have been deployed to look at individual marine algae and to assess population changes more accurately. Grab samples brought to the surface are analyzed using laboratory flow cytometers (Becker et al., 2002; Gerdts and Luedke, 2006). Smaller "personal flow cytometers" such as the Accuri C6 have been brought onto the boats in order to analyze such grab samples at the point of collection, and laboratory instruments have been modified for submersion in relatively shallow waters. Clearly, the opportunity to evaluate algal populations *in situ* is very appealing, and the size, shape, and intrinsic pigment fluorescence provide characteristics that can be measured using flow cytometry without staining or other preprocessing steps. Cell imaging *in situ* is also an exciting area under development, but is currently slow and provides limited resolution for identification (Blaschko et al., 2005; Campbell et al., 2008). The Cytobot and the Cytobuoy instruments are the most notable of the marine flow cytometers already deployed (Dubelaar and Gerritzen, 2000; Takabayashi et al., 2006; Thyssen et al., 2008). While both are large, expensive systems, the latter is commercially available and is producing interesting data on algal populations around the globe (Olson et al., 2003; Takabayashi et al., 2006; Thyssen et al., 2008).

Microflow cytometry offers the potential to provide a much less expensive alternative for underwater deployment than the currently available instruments (Ligler and Kim, 2010). The smaller size and lower power requirement also suggests that a Microflow Cytometer could be deployed on an unmanned underwater vehicle (UUV) for more extensive analyses than a system dragged by a ship or deployed on a buoy. A prototype cytometer has been deployed on an unmanned underwater vehicle, but the vehicle was large with a 100 kg payload capacity (Cunningham et al., 2003). An ideal

* Corresponding author. Tel.: +1 202 404 6002; fax: +1 202 404 8897.
E-mail address: Frances.ligler@nrl.navy.mil (F.S. Ligler).

0956-5663/$ – see front matter. Published by Elsevier B.V.
doi:10.1016/j.bios.2011.03.042

deployable cytometer would be low power, light weight, pressure-resistant, and capable of measuring both size and fluorescence of multiple pigments, including chlorophyll a and phycoerythrin. The Morgan group in Southhampton UK is developing a flow cytometer for measuring phytoplankton that employs impedance instead of light scatter to measure size (Benazzi et al., 2007; Mowlem et al., 2006). They have demonstrated the discrimination of three different marine algae based on fluorescence emission at 585 and 675 nm and impedance at 327 kHz. However, the smallest taxa tested, *Synechococcus*, was too small to produce an impedance signal.

NRL is developing the Microflow Cytometer for monitoring algal population changes on UUVs. The initial prototype uses grooves in the top and bottom of the flow channel to direct the sheath fluid completely around the sample stream. The sheathing of the core using such passive structures has distinct advantages: less chance of clogging, the ability to interrogate both large and small objects, and minimal shear stress due to the distance of the core from the wall. The sheath fluid, with a higher volumetric flow rate, focuses the sample stream in front of the excitation beams for measurement of right angle light scatter and fluorescence. We have already demonstrated the resolution of this device for discriminating fluorescently coded beads in multiplexed immunoassays (Golden et al., 2009; Kim et al., 2009) and the potential for recycling the sheath fluid (Hashemi et al., 2010) in case minimization of sheath fluid volume proves to be desirable in the final system. In order to develop a Microflow Cytometer for discriminating populations of marine algae, however, it is necessary to demonstrate discrimination of different algae based on light scatter, as a rough measure of size, and fluorescence at wavelengths appropriate for intrinsic pigments. We characterized the spectra of three different algal species in order to predict the optimum excitation and emission wavelengths for discrimination using portable lasers. While we evaluated the flow cytometry data at all of these wavelengths, we were particularly interested in comparing data obtained using the Microflow Cytometer to that obtained using the commercial Accuri C6 system being marketed for shipboard applications (Veldhuis, 2010); using identical wavelengths for excitation and emission was critical for this comparison. The Microflow Cytometer prototype was able to distinguish the same algal populations with similar resolution to that achieved using the much larger and more expensive commercial system.

2. Experimental

2.1. Design and fabrication of Microflow Cytometer

The Microflow Cytometer employed sets of chevron-shaped grooves on the top and bottom of a flow channel in order to create sheath flow. This design wraps two symmetric sheath streams around a central core stream as previously demonstrated (Hashemi et al., 2010; Howell et al., 2008). Unlike our previous designs, the sample inlet width was chosen to be 390 μm to prevent destruction of larger phytoplankton species. We optimized the new design based on simulated hydrodynamic focusing and transferred the design to L-Edit commercial software. Glass photomasks were created using a Heidelberg DWL-66 laser pattern generator.

The Microflow Cytometer channels were fabricated in polydimethylsiloxane (PDMS) using standard microfabrication procedures (Hashemi et al., 2010; Howell et al., 2008). Briefly, a master was created on a silicon wafer by sequentially spinning on layers of SU-8 photoresist and exposing with a photomask. After development, the master was placed into the bottom of a mold, and PDMS was poured on top to make layers with thicknesses of approximately 1 mm (bottom) or 10 mm (top). The PDMS was allowed to cure and was then peeled from the master. Fluidic inlets were

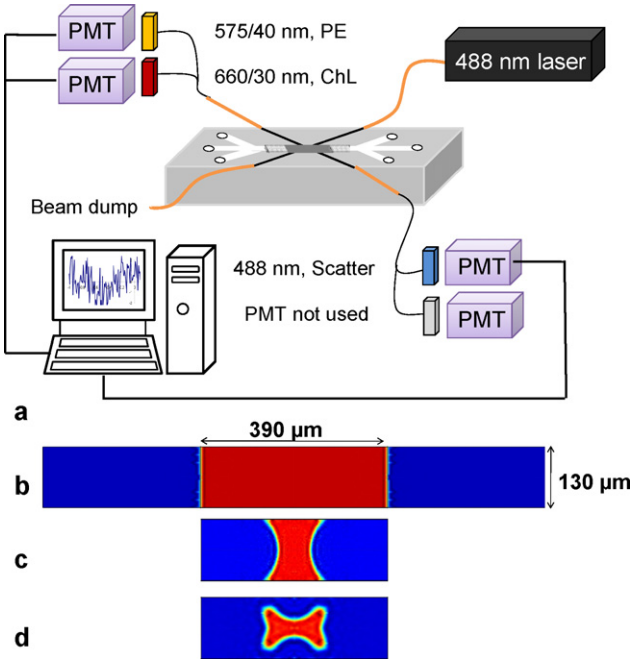

Fig. 1. (a) A schematic of the optical and microfluidics setup. The core fluid and sheath fluid enter the microchannel at flow rates of 200 μL/min and 800 μL/min, respectively. The cross-sections in the simulation were selected at positions that correspond to the locations in the actual microchannel: (b) at inlet to the main channel, (c) immediately before the chevrons where the faster flowing sheath streams have focused the core laterally, and (d) after the chevrons where the core has been compressed vertically.

cored into the top of the cytometer, and polyetheretherketone (PEEK) tubing sections with an internal diameter of 400 μm and a length of 13 mm were placed into the inlets. Channels were 130 μm high throughout and 390 μm wide in the sheathing and interrogation region. The chevron-shaped grooves extended 65 μm into the top and bottom of the channels. The two PDMS pieces were then bonded together by oxygen plasma treatment. Finally, optical fibers were cleaved, placed into their guide channels and carefully aligned with the channel walls.

A schematic of the optical setup is shown in Fig. 1a. Optical excitation at 488 nm was provided by an argon-ion laser (Ion Laser Technologies), which was launched into a multimode optical fiber with a core approximately 65 μm in diameter. The optical fiber delivered excitation light into the interrogation region of the cytometer. A second multimode fiber on the far side of the channel served as a beam dump to prevent excess scattered light in the channel. Fluorescence and light scatter were collected using two multimode optical fibers placed at 90° angles to the beam dump fiber. Light emerging from each collection fiber was directed through a fiber splitter, through a bandpass filter (Omega Optical Inc., Brattleboro, VT), and finally into a photomultiplier tube (PMT, H9307-02, Hamamatsu, Bridgewater, NJ).

COMSOL Multiphysics finite element analysis software (COMSOL Inc., Palo Alto, CA) was used for analysis and optimization of the microchannel at specific core and sheath flow rates. To reduce computation time, the channel was assumed to be symmetrical in both horizontal and vertical directions and only one quadrant of the channel was simulated. The actual core size of 390 μm wide and 130 μm high at the inlet was simulated. Sheath inlets with the same dimensions were simulated on both sides of the core. The simulations in Fig. 1b–d depict the core stream in the main channel at the inlet, before the chevrons, and after the chevrons. In Fig. 1c, the core stream has been compressed laterally by the two incoming sheath streams. In Fig. 1d, the chevrons have redirected the sheath fluid to

Table 1
Characteristics of phytoplankton species used in this study.

	Synechococcus sp. (LB 2380)	*Nitzschia dissipata* (LB FD253)	*Thalassiosira pseudonana* (LB FD2)
Class	Cyanophyceae	Bacillariophyceae	Coscinodiscophyceae
Photosynthetic Pigments	Chlorophyll a Phycobilins – Phycocyanin – Phycoerythrin Carotenoids	Chlorophyll a & c Carotenoids	Chlorophyll a & c Carotenoids
Shape	Spherical or ellipsoidal moves by oscillating Unicellular	Elliptical or elongated frustules isopolar, bilaterally symmetrical solitary cells	Cylindrical valves: circular structures capping the top and bottom of the cylinder Girdle bands: a series of thin silica strips on the sides, unicellular (Hildebrand et al., 2009)
Size	0.8–1.5 μm	12–85 μm in length, 3–6 μm in width	8–32 μm in length, 4–14 μm in width

the top and bottom of the channel and have vertically compressed the core stream. The dimensions of the focused core (Fig. 1d) were measured from the positions where the dye concentration is 0.4, assuming the undiluted dye solution has a fluorescence intensity of 1 and the concentration in the sheath is 0. The width of the core was 131 μm while the height was 38 μm in the center and 87 μm at the outer corners.

A voltage signal was collected from the PMTs, digitized on a 16-bit A/D board (Data Translation Inc.), and sent through a USB cable to a personal computer. The software interface was written using LabWindows (National Instruments). Data was acquired at 200 kilo-samples per second (kSPS) per channel. Since hard drive access is very slow, to avoid A/D card buffer overflows and dropped data points, we implemented data thresholding and a modified data storage procedure. Data was recorded only when the signal from the scatter channel was above threshold, greatly reducing the amount of data to be stored. If the scatter signal rose above threshold, the computer added a timestamp and transferred the data to memory allocated in RAM. Testing indicated that no data was dropped between buffer fills. Only after the experiment was completed was data transferred from RAM onto the hard drive. Although such a data collection system can operate at very high bandwidths, there was a danger that the RAM could overflow, especially if the threshold voltage was set too low. Four channels of continuously recorded 16-bit data from PMTs collected at 200 kSPS filled approximately one GB of RAM in about 8 min. Since the longest experiment required 5 min, and the computer contained several GB of RAM, the danger of memory overflow was eliminated when the setup is used as designed.

2.2. Microflow Cytometer operation

The sample was injected into the channel using a precision syringe pump (CAVRO XE 1000, Tecan Systems Inc., San Jose, CA) at a flow rate of 200 μL/min. The pump was controlled with software written in Lab-Windows/CVI via RS232 communication. A bidirectional peristaltic pump (P625/66.143, Instech Laboratories Inc., Plymouth, PA) was used to introduce the sheath flow into the channel. The sheath flow rate was 800 μL/min.

PMT gains for the detection of fluorescent characteristics of the phytoplankton were set to 0.95 V and for the detection of light scatter were set to 0.65 V. Data from three PMTs at 488 ±5 nm (light scatter), 660 ± 30 nm (chlorophyll), and 575 ± 40 nm (phycoerythrin) was collected and stored using the acquisition software. The sampling frequency was set to 200 kSPS. A light scatter threshold of 0.005 V was set in the data acquisition software to trigger data collection of each event (each microorganism passing through the interrogation region). The data acquisition software registered an event when the light scatter exceeded the threshold level and the data from two fluorescent channels and side scatter were recorded. Data analysis software correlated the signals detected for each microorganism passing through the interrogation region and created scatter plots of fluorescence vs. side scatter. The mean chlorophyll and phycoerythrin fluorescence, as well as light scatter data were determined for each phytoplankton population and compared.

2.3. Phytoplanktonic species

Cultures of the three different algae were purchased from the Culture Collection of Algae (UTEX, Austin, TX). More information about the cultures is supplied in ESI. There are three classes of pigments present in these algae: chlorophylls, phycobilins, and carotenoids. Chlorophyll is a green pigment present in all phytoplankton, plants and cyanobacteria and can be used to discriminate phytoplankton from most other marine particles in a similar size range. Chlorophyll a is the primary photosynthetic pigment with a maximum absorption at 675 nm; however, chlorophyll also absorbs

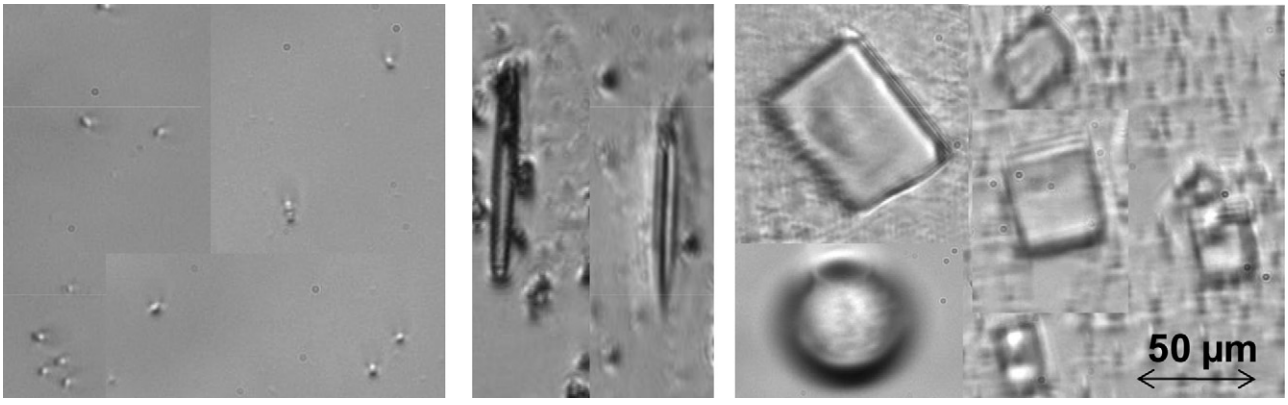

Fig. 2. Microscopy of the phytoplankton species. The photos show representative images of *Synechococcus* sp. (left) and *Nitzschia d.* (middle). Due to the greater spacing between individual cells, a collage of images of *Thalassiosira p.* is included (right).

well at ~450 nm. Chlorophyll c couples photonic energy to chlorophyll a and is found in diatoms and dinoflagellates. Phycocyanin and phycoerythrin are present in cyanobacteria; phycoerythrin absorbs at 495 and 545–565 nm and fluoresces at 575 nm. Carotenoids are lipid-soluble pigments absorbing light in the blue to cyan region of approximately 450–490 nm. The phytoplanktonic species used for this work are shown in Table 1.

Prior to introduction into the Microflow Cytometer or Accuri C6, the algae were gently stirred to dissociate aggregates. Observation of the stirred samples under the microscope confirmed that most of the aggregates were dispersed and that there was visible heterogeneity among the cells in each population.

3. Results and discussion

3.1. Phytoplankton characterization

A Nikon Eclipse TE2000U inverted microscope was used to image the three phytoplankton species. The cell dimensions were found to be in the range of 0.5–1.0 μm in diameter for *Synechococcus* sp., 16–80 μm in length and 2–5 μm in width for *Nitzschia d.*, and 8–38 μm in length and 4–29 μm in width for *Thalassiosira p.* Bright field photographs of each microorganism are shown in Fig. 2.

Each phytoplankton species also produced distinctive fluorescent emission spectra as a result of different pigment concentrations. Using a TECAN Spectrophotometer (Tecan Trading AG, Switzerland) and 488 nm excitation, the emission spectra of each of the three algal species was collected (Fig. 3a). When excited with a 488 nm laser, the fluorescence emission spectrum showed that *Synechococcus* sp. emitted strongly in the red region (640–700 nm) with a smaller peak at 545 nm. *Nitzschia d.* and *Thalassiosira p.* both had strong peaks at 540–545 nm (in the green region), and *Thalassiosira p.* showed a smaller peak at 680 nm as well. For comparison of the cell spectra with purified pigments, Fig. 3b shows the emission spectra for R-phycoerythrin (AnaSpec Inc., Fremont, CA) and chlorophyll purified from *Dinophyceae* (Jackson ImmunoResearch Laboratories Inc., West Grove, PA) excited with 488 nm light.

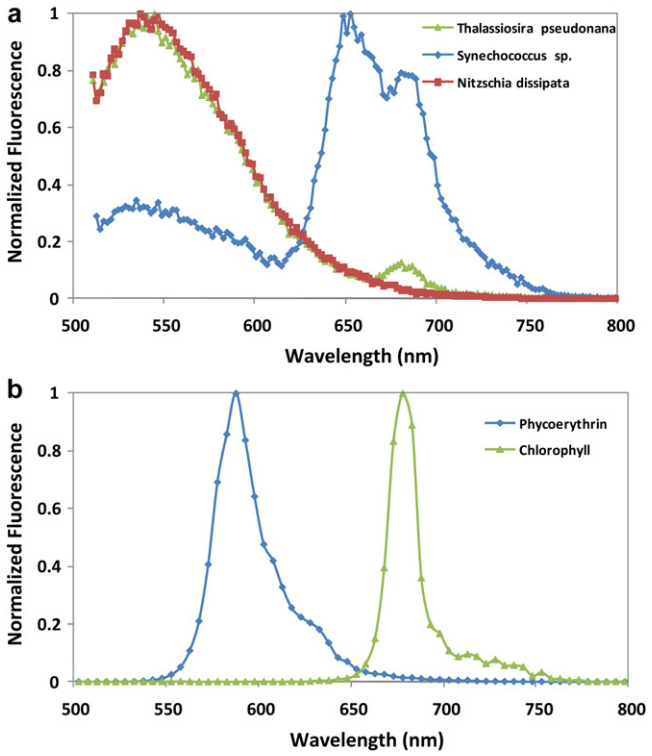

Fig. 3. Fluorescence emission spectra of (a) the three algal species and (b) the phycoerythrin and chlorophyll excited with 488 nm light.

3.2. Flow cytometry of phytoplankton

The phytoplankton species were analyzed using the Microflow Cytometer and an Accuri C6 flow cytometer (Ann Arbor, MI). The concentration of the phytoplankton flowing through both Microflow Cytometers was ~2100 cells/μL for the *Synechococcus* sp., ~50 cells/μL for the *Nitzschia d.*, and ~150 cells/μL for the *Thalassiosira p.* The excitation and emission wavelengths for the various pigments found in phytoplankton compared to the excitation and emission wavelengths used by the flow cytometers in this analysis are summarized in Table S1 in the ESI. Chlorophyll a is not strongly excited at 488 nm. However, there is enough excitation to observe a significant fluorescence signal in the wavelengths longer than 650 nm. Phycoerythrin is excited by the 488 nm laser and detected at ~585 nm. Although the 488 nm excitation was not optimal for exciting the pigments, this wavelength did excite both chlorophyll and phycoerythrin, providing a basis for comparison of characterization data from the two instruments.

Fig. 4a and b show scattergrams of the magnitude of the phycoerythrin fluorescence (575–585 nm) plotted vs. chlorophyll fluorescence (650–680 nm). Fig. 4a shows the fluorescence data obtained using the Microflow Cytometer and Fig. 4b depicts the fluorescence data obtained by the Accuri flow cytometer. The data shows that the three different populations can be discriminated based on their fluorescence emission spectrum in both systems. The correlation between the two data sets was found to be very similar statistically as shown later in Table 2. *Nitzschia d.* emits strongly in the orange region (characteristic of phycoerythrin), while the red fluorescence (characteristic of chlorophyll) is very weak. *Thalassiosira p.* emits most strongly in the red region consistent with the smaller peak (660–690 nm) seen in Fig. 3a. However, it does not emit as strongly in the orange region. *Synechococcus* sp. emits both in the red and orange spectrum.

Table 2
Statistical analysis of data collected using the Accuri C6 and the Microflow Cytometer.

	Mean SSC[a]	CV SSC (%)	Mean Chl.[a]	CV Chl. (%)	Mean PE[a]	CV PE (%)	Mean PE/Chl.
Accuri C6							
Synechococcus sp.	4.0	202	9.4	100	0.28	180	0.06
Nitzschia d.	570	103	7.0	240	2.3	320	31
Thalassiosira p.	12	291	86	53	0.10	71	0.015
Microflow Cytometer							
Synechococcus sp.	9.8	235	23	260	0.46	200	0.04
Nitzschia d.	160	101	3.9	120	9.7	110	2.6
Thalassiosira p.	31	163	75	86	0.25	89	0.005

[a] PMT values are arbitrary optical units. All mean intensities for the Accuri can be multiplied by 10^4 and the numbers for the Microflow Cytometer by 10^{-1} to get the raw numbers shown on the dot plots. The mean PE/Chl. ratios are dimensionless.

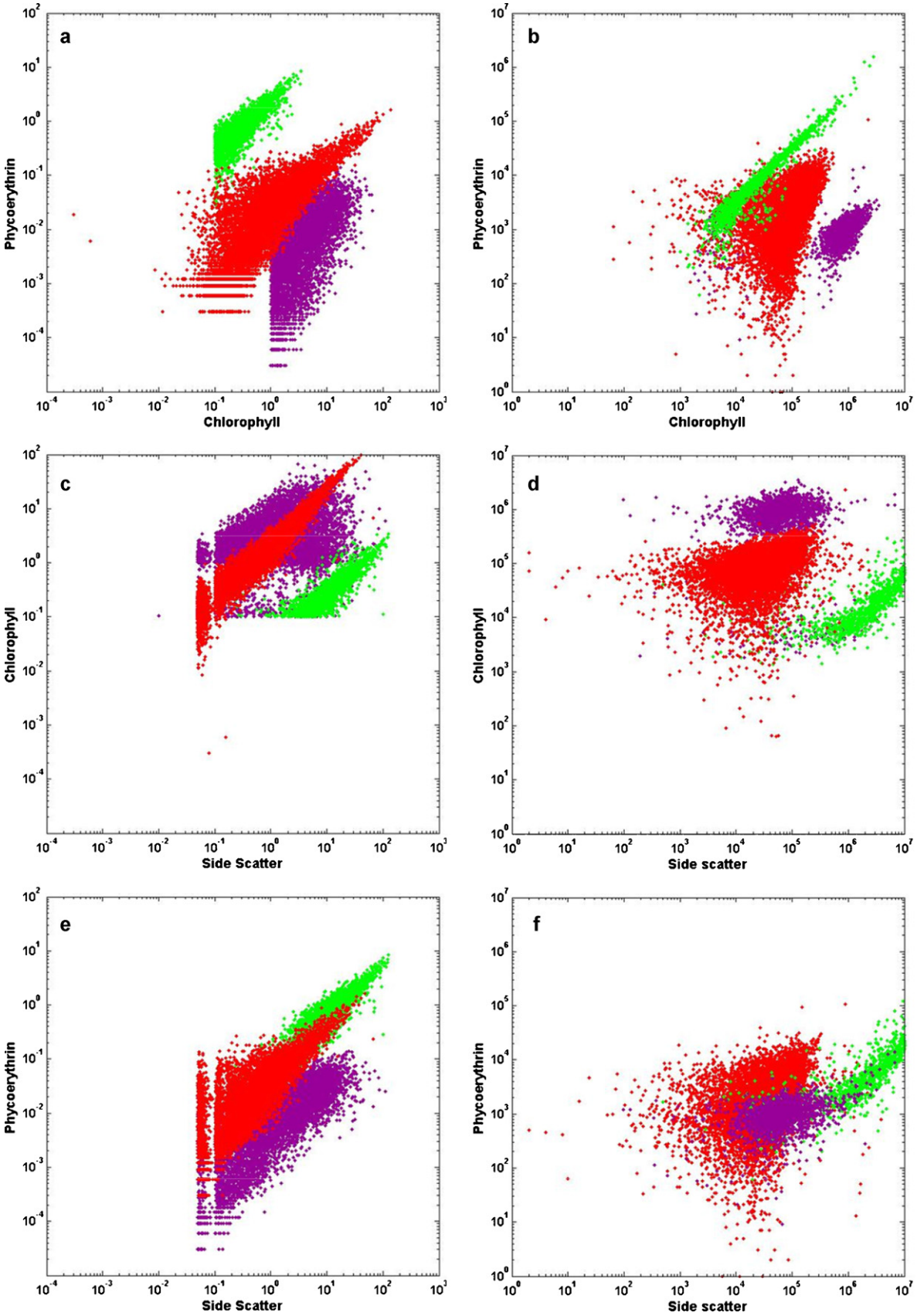

Fig. 4. Scatter plots of the phycoerythrin (*y*-axis) plotted vs. chlorophyll fluorescence (*x*-axis) for each individual cell are shown in (a and b). (c and d) depict scatter plots of chlorophyll fluorescence vs. side scatter, and (e and f) represent scatter plots of phycoerythrin fluorescence vs. side scatter. (a, c, and e) are the data obtained using the Microflow Cytometer and (b, d, and f) show the Accuri flow cytometer results. *Synechococcus* sp. is represented by red dots, *Nitzschia d.* by green dots, and *Thalassiosira p.* by purple dots. (For interpretation of the references to color in this figure legend, the reader is referred to the web version of the article.)

Scattergrams of chlorophyll fluorescence vs. side scatter (488 nm) and phycoerythrin fluorescence vs. side scatter are shown in Fig. 4c–f. The side scatter data is the largest for *Nitzschia d.* and the smallest for *Synechococcus* sp. The proportional increase of both pigments as the light scatter increases for *Synechococcus* suggests that the particles with higher side scatter may be aggregates. The same could be true for *Nitzschia d.*, but the individual cells are clearly larger.

The statistical data obtained using the Accuri and the Microflow Cytometer are summarized in Table 2. The mean values were used to provide a comparison between the different cell populations. The coefficient of variation (CV) was calculated for each of the different parameters presented in Fig. 4 in order to obtain a metric for the heterogeneity of each cell population.

In general, larger particles produce larger side scatter signal than smaller ones in both cytometers; but there was not an exact correlation. Volten and colleagues found that the Mie theory (based on sphericity and homogeneity) did not produce good approximations of scattering by phytoplankton, due to differences in internal structure and inclusions (Volten et al., 1998). The Accuri produced a mean value of side scatter on the order of 4.0×10^4 for *Synechococcus* sp. that increased one order of magnitude for *Thalassiosira p.* and two orders of magnitude for *Nitzschia d.* Data from our instrument also showed the smallest side scatter value of 0.98 for the *Synechococcus* sp. ($\sim$1.0 μm in diameter) and the largest value of 16 for the *Nitzschia d.* ($\leq$80 μm long). In both cases, the mean value for *Thalassiosira p.* was three times that for *Synechococcus* sp., while the *Nitzschia d.* was much larger. This observation was also consistent with the observed sizes of the species obtained by microscopy. The CVs were high for all measurements, reflecting the heterogeneity of the cell populations as seen in the microscope images.

Mean chlorophyll intensity was found to be the lowest for the *Nitzschia d*. and the highest for the *Thalassiosira p.* in both cytometers. The CV for the fluorescence of chlorophyll for the *Thalassiosira p.* was the smallest among all the species studied. While the largest CV for chlorophyll was found for the *Nitzschia d*. using the Accuri, CV for chlorophyll fluorescence was the largest for the *Synechococcus* sp. using the Microflow Cytometer. In both cytometers, the mean intensity of phycoerythrin for both *Thalassiosira p.* and *Synechococcus* sp. was about an order of magnitude less than for *Nitzschia d*. and the CVs were about the same for both systems. However, the Microflow Cytometer showed a significantly smaller CV for all signals for the *Nitzschia d*. in comparison with the Accuri flow cytometer. The PE/Chl. ratio was calculated based on the ratio of phycoerythrin to chlorophyll for each individual cell. The ratios of phycoerythrin to chlorophyll (PE/Chl.) were found to be the largest for *Nitzschia d*. and the smallest for *Thalassiosira p.* in both systems.

4. Conclusions

We have designed and developed a Microflow Cytometer that measures light scatter and fluorescence properties of microorganisms. We used our instrument to characterize and discriminate three populations of phytoplankton. The phytoplankton were resolved on the basis of side scatter and multi-wavelength fluorescence. The Microflow Cytometer results were comparable with the results obtained using Accuri C6 flow cytometer. Our system is sensitive enough to characterize and detect the picoplankton *Synechococcus* sp. with diameter less than 1 μm and is also capable of measuring phytoplankton species as long as 80 μm (*Nitzschia d.*). The wide range of cell sizes measurable using the Microflow Cytometer is very significant. Now that we have established the validity of our results by comparison to a more conventional cytometer, we are replacing the large 488 nm argon laser with solid-state lasers that are both small for *in situ* use and provide excitation light closer to maximum absorbance wavelengths for chlorophyll and phycoerythrin (Hashemi et al., 2011). This system can thus be miniaturized and adapted for deployment on unmanned underwater vehicles.

Acknowledgements

This work was supported by ONR/NRL 6.2 work unit 69-6339. Nastaran Hashemi is an American Society for Engineering Education (ASEE) Postdoctoral Fellow. Kirsten Jackson was a Navy Research Enterprise Internship Program summer fellow. The authors thank Dr. Alan Weidemann (Naval Research Laboratory, Stennis, MI) and Dr. Lisa Hilliard (National Oceanic and Atmospheric Administration, Charleston, SC) for their assistance with this project. The views expressed here are those of the authors and do not represent opinion or policy of the US Navy or Department of Defense.

Appendix A. Supplementary data

Supplementary data associated with this article can be found, in the online version, at doi:10.1016/j.bios.2011.03.042.

References

Barbini, R., Colao, F., Fantoni, R., Fiorani, L., Kolodnikova, N.V., Palucci, A., 2006. Annals of Geophysics 49 (1), 35–43.
Becker, A., Meister, A., Wilhelm, C., 2002. Cytometry 48 (1), 45–57.
Benazzi, G., Holmes, D., Sun, T., Mowlem, M.C., Morgan, H., 2007. IET Nanobiotechnology 1 (6), 94–101.
Blaschko, M.B., Holness, G., Mattar, M.A., Lisin, D., Utgoff, P.E., Hanson, A.R., Schultz, H., Riseman, E.M., Sieracki, M.E., Balch, W.M., Tupper, B., 2005. In: Seventh IEEE Workshop on Applications of Computer Vision, pp. 79–86.
Burk, C., Usleber, E., Martlbauer, E., 1998. Archiv Fur Lebensmittelhygiene 49 (1), 16–20.
Campbell, L., Walpert, J.N., Guinasso, N.L., 2008. Nova Hedwigia, 161.
Churnside, J.H., Donaghay, P.L., 2009. ICES Journal of Marine Science 66 (4), 778–789.
Cunningham, A., McKee, D., Craig, S., Tarran, G., Widdicombe, C., 2003. Journal of Marine Systems 43 (1–2), 51–59.
Drozdowska, V., 2007. Oceanologia 49 (1), 59–69.
Dubelaar, G.B.J., Gerritzen, P.L., 2000. Scientia Marina 64 (2), 255–265.
Fantoni, R., Fiorani, L., Okladnikov, I.G., Palucci, A., 2006. In: Frenz, M., Larichev, A.V., Matvienko, G.G., Panchenko, V.Y., Singh, U.N. (Eds.), International Conference on Lasers, Applications, and Technologies 2005: Laser Technologies for Environmental Monitoring and Ecological Applications and Laser Technologies for Medicine, pp. 28402–28402.
Fiorani, L., Okladnikov, I.G., Palucci, A., 2007. Journal of Optoelectronics and Advanced Materials 9 (12), 3939–3945.
Gerdts, G., Luedke, G., 2006. Journal of Microbiological Methods 64 (2), 232–240.
Golden, J.P., Kim, J.S., Erickson, J.S., Hilliard, L.R., Howell, P.B., Anderson, G.P., Nasir, M., Ligler, F.S., 2009. Lab on a Chip 9 (13), 1942–1950.
Harvell, C.D., Kim, K., Burkholder, J.M., Colwell, R.R., Epstein, P.R., Grimes, D.J., Hofmann, E.E., Lipp, E.K., Osterhaus, A., Overstreet, R.M., Porter, J.W., Smith, G.W., Vasta, G.R., 1999. Science 285 (5433), 1505–1510.
Hashemi, N., Howell Jr., P., Erickson, J., Golden, J., Ligler, F., 2010. Lab on a Chip 10 (15), 1952–1959.
Hashemi, N., Erickson, J., Golden, J., Ligler, F., 2011. Optofluidic characterization of marine algae using a microflow cytometer. Biomicrofluidics, in press.
Hildebrand, M., Kim, S., Shi, D., Scott, K., Subramaniam, S., 2009. Journal of Structural Biology 166 (3), 316–328.
Hoge, F.E., Lyon, P.E., Wright, C.W., Swift, R.N., Yungel, J.K., 2005. Applied Optics 44 (14), 2857–2862.
Howell Jr., P.B., Golden, J.P., Hilliard, L.R., Erickson, J.S., Mott, D.R., Ligler, F.S., 2008. Lab on a Chip 8 (7), 1097–1103.
Kim, J.S., Anderson, G.P., Erickson, J.S., Golden, J.P., Nasir, M., Ligler, F.S., 2009. Analytical Chemistry 81 (13), 5426–5432.
Knap, A., Dewailly, E., Furgal, C., Galvin, J., Baden, D., Bowen, R.E., Depledge, M., Duguay, L., Fleming, L.E., Ford, T., Moser, F., Owen, R., Suk, W.A., Unluata, U., 2002. Environmental Health Perspectives 110 (9), 839–845.
Landsberg, J.H., 2002. Reviews in Fisheries Science 10 (2), 113–390.
Ligler, F.S., Kim, J.S. (Eds.), 2010. The Microflow Cytometer. PanStanford Publishing, Singapore, p. 379.
Mowlem, M., Chavagnac, V., Statham, P., Burkill, P., Benazzi, G., Holmes, D., Morgan, H., Haas, C., Kraft, M., Taberham, A., 2006. Oceans 2006 1–4, 845–850.
Nehring, S., 1998. ICES Journal of Marine Science 55 (4), 818–823.
Olson, R.J., Shalapyonok, A., Sosik, H.M., 2003. Deep-Sea Research Part I – Oceanographic Research Papers 50 (2), 301–315.

Takabayashi, M., Lew, K., Johnson, A., Marchi, A., Dugdale, R., Wilkerson, F.P., 2006. Journal of Plankton Research 28 (9), 831–840.
Thyssen, M., Mathieu, D., Garcia, N., Denis, M., 2008. Journal of Plankton Research 30 (9), 1027–1040.
Veldhuis, M., 2010. http://www.accuricytometers.com/technical_information/white-papers/aquatic-research-white-paper/.
Volten, H., de Haan, J.F., Hovenier, J.W., Schreurs, R., Vassen, W., Dekker, A.G., Hoogenboom, H.J., Charlton, F., Wouts, R., 1998. Limnology and Oceanography 43 (6), 1180–1197.